sustainability

MDPI

Article

Detection Method for All Types of Traffic Conflicts in Work Zones

Zhepu Xu * and Dashan Chen

Department of Railway Transportation, Shanghai Institute of Technology, Shanghai 201418, China
* Correspondence: xuzhepu@126.com

Abstract: Traffic conflict technology (TCT) is widely used to assess the safety of work zones. The current TCT is temporal and (or) spatial proximity defined based, which can only detect two-vehicle or multi-vehicle conflicts, and is not competent for single-vehicle conflicts. However, single-vehicle accidents in work zones are also severe. This study proposes a detection method for all types of traffic conflicts in work zones. Based on vehicle micro-behavior data, evasive behavior is detected by automatic segmentation, Support Vector Machine (SVM)-based behavior identification, and threshold-based judgment methods. Two-vehicle or multi-vehicle conflicts are detected by classical proximity defined-based method, i.e., the surrogate safety assessment model (SSAM). By comparing the analysis results of the evasive behavior with the one of SSAM, single-vehicle conflicts can be detected. Taking a practical work zone as an example, the effectiveness of this method in detecting all types of traffic conflicts in work zones is verified. The single-vehicle conflict can be subdivided into 10 types according to basic behavior types, such as straight-line driving and decelerating. The two or multi-vehicle conflicts can be subdivided into three types, such as rear-end conflict. The example also verifies the applicability of this method under different traffic volume scenarios.

Keywords: traffic conflict; safety assessment; work zone; surrogate safety assessment model (SSAM); evasive behavior; traffic conflict technology (TCT)

check for updates

Citation: Xu, Z.; Chen, D. Detection Method for All Types of Traffic Conflicts in Work Zones. *Sustainability* **2022**, *14*, 14159. https://doi.org/10.3390/su142114159

Academic Editor: Elżbieta Macioszek

Received: 26 September 2022
Accepted: 27 October 2022
Published: 30 October 2022

Publisher's Note: MDPI stays neutral with regard to jurisdictional claims in published maps and institutional affiliations.

Copyright: © 2022 by the authors. Licensee MDPI, Basel, Switzerland. This article is an open access article distributed under the terms and conditions of the Creative Commons Attribution (CC BY) license (https://creativecommons.org/licenses/by/4.0/).

1. Introduction

As the road network enters the maintenance era, more road works will occur. The setting of work zones will make the vehicle operating environment more complex and can easily lead to traffic accidents. Safety assessment for work zones is attracting the attention of researchers.

How to assess the safety of a work zone? The most direct way is to see whether there are traffic accidents in the work zone, and the number of them. This method has high requirements on accident records, but accident records are lagging, so only post-assessment can be performed. Besides, many countries or regions have not established a complete accident record mechanism, which makes this method difficult to be promoted [1].

Recognizing the above problems, researchers have put forward some surrogate indicators, among which the most known is traffic conflict, which occurs frequently, is easier to be observed than accidents, and thus has been widely used. Traffic conflicts can also reflect the safety level of the work zone to a certain extent. The more traffic conflicts, the less safe they are. The critical content of traffic conflict technology (TCT) is the detection of traffic conflict, which is the main focus of this paper.

Historically, different definitions of traffic conflict were proposed, mainly based on proximity and evasive behavior. In the past, restricted by the means of data collection, the definition based on evasive behavior gradually faded out of vision. In contrast, the definition based on proximity has now become the mainstream definition. Many traffic conflict indicators have been proposed based on the definition of proximity. However, these indicators mainly focus on the conflict between two or more vehicles (e.g., rear-end conflict,

lane change conflict). They cannot detect single-vehicle conflict (e.g., running off-road, striking fixed objects).

Accident data shows that although the most common accident type in work zones is rear-end collision, single-vehicle accidents cannot be underestimated. The analysis of accidents in work zones from 2006 to 2020 in the FARS (Fatality Analysis Reporting System) database of the U.S. National Highway Traffic Safety Administration shows that: (1) a total of 9905 fatal motor vehicle crashes occurred, of which 4897 were single vehicle accidents, accounting for 49%; (2) a total of 5,325,340 estimated injury only motor vehicle crashes occurred, of which 1,709,985 were single vehicle accidents, accounting for 32%; and (3) a total of 13,310,524 estimated property damage only (PDO) motor vehicle crashes occurred, of which 4,108,292 were single vehicle accidents, accounting for 31%. It can be seen that the single-vehicle accident is a vital accident type in work zones, and the death rate among single-vehicle accidents is high. However, existing research on the safety of work zones mainly focuses on two or multi-vehicle accidents, and attention to single-vehicle accidents is far from ideal.

Our previous research [2] found that the definition of traffic conflict, based on evasive behavior, has the connotation of single-vehicle conflict and can effectively deal with detecting single-vehicle conflict. This definition's key is in obtaining the micro-behavior data of vehicles in the work zone. Thanks to the progress of technology, these data can be obtained easily, which brings new hope to applying traffic conflict based on the definition of evasive behavior. The originality and contribution of this paper is two-fold: (1) by reviewing the definition of traffic conflict based on evasive behavior and combining the two definitions, a method that can detect all types of traffic conflict is proposed, including single-vehicle, two, and multi-vehicle conflicts; and (2) it realizes the full automation of conflict detection and can efficiently complete the detection of all types of traffic conflicts based on the trajectory data obtained from microscopic traffic simulation and actual measurement, laying a good foundation for the fast safety assessment for work zones.

The remainder of this paper is arranged as follows: Section 2 consists of a research review including TCT based on two different definitions and advanced data acquisition technologies for collecting micro-behavior data, which is the basis for detecting traffic conflicts. Section 3 presents the detection method for all types of traffic conflicts. Section 4 contains an example used to demonstrate the implementation and effect of this method. The paper is concluded in Section 5, consisting of the summary and remarks for further research.

2. Research Review

2.1. Traffic Conflict Technology

2.1.1. Definition Based on Proximity

At the first traffic conflict conference in 1977, Amundsen and Hyden proposed the classic definition of traffic conflict based on proximity, which was later widely recognized. A traffic conflict is an observable situation in which two or more road users approach each other in space and time to such an extent that there is a risk of collision if their movements remain unchanged [1]. Researchers have proposed various indicators to quantify road users' proximity based on this definition. These indicators are roughly divided into three categories [3]: (1) indicators based on temporal proximity, such as TTC (time to collision); (2) indicators based on spatial proximity, such as PSD (proportion of stopping distance); and (3) indicators derived from the above two indicators, such as DRAC (deceleration rate to avoid the crash).

As the definition shows, it mainly focuses on two or multi-vehicle conflicts. Therefore, this method is more suitable for the safety assessment of road facilities where a large number of two or multi-vehicle conflicts can be observed. The most typical application scenario is intersections [4]. The successful application of TCT in intersection safety assessment also inspired researchers to try to promote it in work zones [5–7].

However, due to the significant differences between intersections and work zones, there are still some deficiencies in the existing assessment methods, mainly in the following aspects:

(1) The safety assessment for intersections mainly focuses on the conflict between two or multi vehicles. In contrast, for work zones, the single-vehicle accident is also severe due to the change in spatial layout. However, the existing TCT is not competent in detecting single-vehicle conflict. Some researchers have also noticed this problem. Zheng, Ismail, and Meng [3], and Mahmud and Ferreira [8], all pointed out that the existing studies are basically aimed at two or multi-vehicle conflicts and pay no attention to the problem of single-vehicle conflicts. They call on researchers to pay attention to the problem of single-vehicle conflict. Interestingly, in the literature [9], although the author recognizes the existence of single-vehicle conflict, they pointed out that considering the small number of single-vehicle conflicts compared with multi-vehicle conflicts, it would not be considered in the research. This treatment may be feasible in intersection safety assessment, but may be a great hidden danger in work zones. Besides, some researchers are pessimistic about applying proximity-defined-based TCT in single-vehicle conflict assessment. They believe that this technology is the one to describe the risk degree of mutual interference between multiple traffic participants, and does not include the dangerous state of a single traffic object and the disharmony between vehicles and roads. Therefore, TCT cannot be used in single-vehicle accident research [10]. Besides, from the point of view of these researchers, it can be seen that the application of proximity-defined based TCT in single-vehicle conflict scenarios is facing great challenges.

(2) Traffic volume at an intersection is generally large. Thus, enough traffic conflicts can be observed. However, road work will be especially carried out during a period with relatively small traffic volume. Especially now, many departments are promoting night construction and trying to avoid a long traffic volume period. Traffic conflict between two or multiple vehicles is difficult to observe, whereas single-vehicle accident at night is more serious. The problem that the existing TCT cannot detect single-vehicle conflict is more prominent in this scenario.

2.1.2. Definition Based on Evasive Behavior

In fact, in the early stage, there was another definition of traffic conflict: a traffic conflict is a phenomenon in which a road user must take evasive behavior (e.g., lane changing, braking, etc.) to avoid collision [11]. Obviously, the definition does not emphasize the number of conflict participants but only the evasive behavior of the road user. Therefore, it covers the scenario of single-vehicle conflict. However, unlike the first definition that various temporal (and (or) spatial) proximity-based indicators can be proposed, it is difficult to put forward the observation indicators of evasive behavior. In particular, in the past, when early data collection means were insufficient, data could only be collected manually. Usually, observable phenomena such as the brake light coming on or a sudden change of driving direction and lane, are used as a reference, and the evasive behavior is judged by experience, which is relatively subjective [8].

With the progress of technology, the application of this definition has ushered in new hope. With the help of advanced data acquisition technologies, micro-behavior data of vehicles (including vehicle trajectory, real-time speed, acceleration, etc.) can be easily obtained. By defining vehicle behavior and evasive behavior, traffic conflicts can be detected using objective indicators and fully automated. A typical development is to use acceleration to characterize evasive behavior. For example, Ishak and Qi [12] obtained the acceleration data of the vehicle based on Vissim simulation and used deceleration to characterize the evasive behavior of the vehicle. Zaki and Sayed et al. used video detection [13], whereas Bagdadi and Varhelyi collected acceleration data based on naturalistic driving methods [14]. They all define evasive behavior based on jerk (i.e., the derivative of acceleration) and found that it has an obvious relationship with accidents.

2.2. Data Acquisition Technologies

Both proximity and evasive behavior defined-based traffic conflict detection methods rely on acquiring fine micro-behavior data of vehicles. Recent advancements in technology allow the collection of a large amount of micro-behavior data. The three most promising methods for data acquisition are video detection, naturalistic driving, and simulation [15].

Video detection-based data acquisition is to record the traffic video using a camera, then use computer vision to extract vehicle data from the video, including traffic volume, speed, trajectory, and other micro-behavior data [16–20]. For example, Zhang used cameras to record traffic video at intersections and the computer vision method to extract the vehicle's trajectory, acceleration, and other data, and then conducted traffic conflict analysis to evaluate traffic safety based on the data extracted [17]. For the monitoring and data collection of short road sections and intersections, this method is relatively proven. However, the work zone has its unique characteristics. The work zone is strip-shaped, and the traditional single-camera method cannot cover the entire work zone. Fortunately, with the development of video stitching and multi-camera detecting technologies, large-scale monitoring problems have been solved [21], which brings us new hope for collecting micro-behavior data in work zones.

Naturalistic driving is carried out by installing data acquisition devices on the vehicle and collecting behavior data of the vehicle or driver in a naturalistic state without disturbing the driver's normal driving [22]. This method is often used in driving behavior-related research, and the scale is increasing [23–25]. Traditional naturalistic driving study installs a large number of sensors in the vehicle. Due to the complicated installation procedure and high installation cost, the vehicles participating in naturalistic driving studies are limited, especially when compared with the cars running on the road daily. The number of instrumented vehicles, in other words, the sample rate is too low; thus, the persuasion of the research results is debatable. In recent years, simplifying naturalistic driving devices, especially portable ones, has become a new trend [26–28]. Johnson and Trivedi [27] used the smartphone as a collection device and adopted a crowd-sourced model for mass data collection. Xu and Yang developed a portable vehicle behavior acquisition device, which can collect the behavior data of all vehicles running on the expressway with the aid of highway toll cards for data collection [2].

With the development of microscopic traffic simulation technology, researchers began to explore using simulation technology to collect data. Simulation software, such as Vissim, can output complete data, supporting researchers in carrying out traffic conflict-related research from multiple aspects [4,29]. The most influential research on traffic conflict analysis based on microscopic simulation platform data is the SSAM (surrogate safety assessment model) [9]. This method combines the traffic simulation model with the conflict analysis algorithm, wherein the algorithm uses the vehicle trajectory data generated by the simulation model to identify the traffic conflict. The software can provide visual analysis results of the conflicts' number, type, severity, and location. Since its release, many researchers at home and abroad have conducted relevant research based on the SSAM [30,31].

2.3. Summary

Using the proximity-defined-based TCT, the problem of two and multi-vehicle conflict detection has been successfully solved and used in the safety assessment of work zones. However, single-vehicle conflict in work zones is also severe. The proximity-defined-based TCT cannot detect single vehicle conflict, and there are safety hazards. The definition of traffic conflict based on evasive behavior has the connotation of single-vehicle conflict, and the progress of data acquisition technology brings new hope for applying this definition. Therefore, this paper reviews three methods that can obtain vehicle micro-behavior data, i.e., methods based on video detection, naturalistic driving, and simulation, which can be used as solid support for traffic conflict detection. Based on these data acquisition methods

and the above two definitions of traffic conflict, this paper proposes a detection method for all types of traffic conflicts in work zones.

3. Methodology

The main content and technical route of this research are shown in Figure 1. According to the actual situation, select the appropriate method to collect the vehicle micro-behavior data and then analyze the traffic conflicts of all types. In this research, "all types" refers to single-vehicle conflict, two and multi-vehicle conflict, wherein two and multi-vehicle conflict detection can be solved by proximity-defined based TCT. In contrast, the single-vehicle conflict needs to be detected by evasive behavior-defined-based TCT.

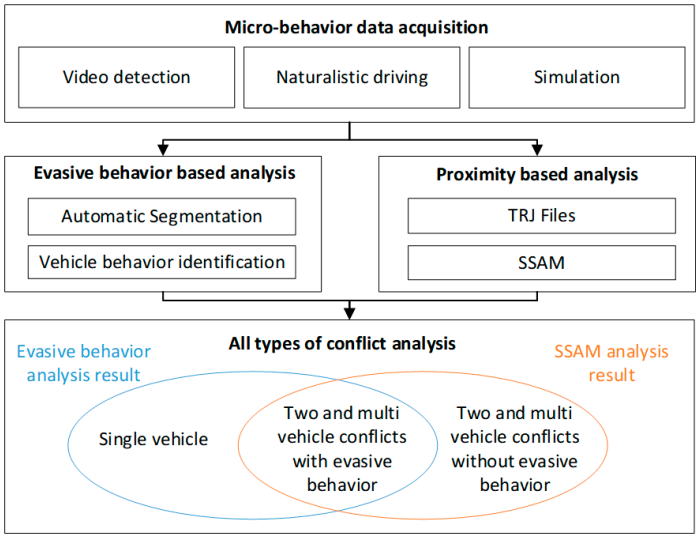


Figure 1. The main content and technical route of this research.

The definition of traffic conflict based on evasive behavior holds that when a vehicle undergoes evasive behavior, it can be recognized as a conflict. However, this includes both single-vehicle conflict and two and multi-vehicle conflict scenarios. To identify the exact conflict type, the method used in this research is as follows:

Conduct conflict detection based on the definition of evasive behavior (including single-vehicle conflict, two and multi-vehicle conflict) and proximity (only including two and multi-vehicle conflict), respectively. Then, analyze the two sets of detection results. If the conflict segment based on evasive behavior analysis is also in the result of proximity-defined-based analysis, then this segment belongs to two or multi-vehicle conflict. Otherwise, it is a single-vehicle conflict.

Next, all types of conflict detection methods proposed in this paper will be introduced in three parts: (1) evasive behavior-based analysis, (2) proximity-based analysis, and (3) all types of conflict analysis.

3.1. Evasive Behavior-Based Analysis

The basis of evasive behavior analysis is the expression of vehicle behavior. Vehicle behavior refers to the vehicle's reaction to the comprehensive action of the driver, the vehicle, and the environment, such as linear acceleration, linear deceleration, and turning. Complex vehicle behavior is composed of basic vehicle behaviors. The following 11 basic vehicle behaviors (as shown in Figure 2) are considered in this study: (1) turning left with constant speed (TL&C); (2) turning left and decelerating (TL&D); (3) turning left and accelerating (TL&A); (4) straight line driving with constant speed (L&C); (5) straight line driving and decelerating (L&D); (6) straight line driving and accelerating (L&A); (7) turning right with constant speed (TR&C); (8) turning right and decelerating (TR&D); (9) turning

right and accelerating (TR&A); (10) lane change to the right (TR&CL); and (11) lane change to the left (TL&CL).

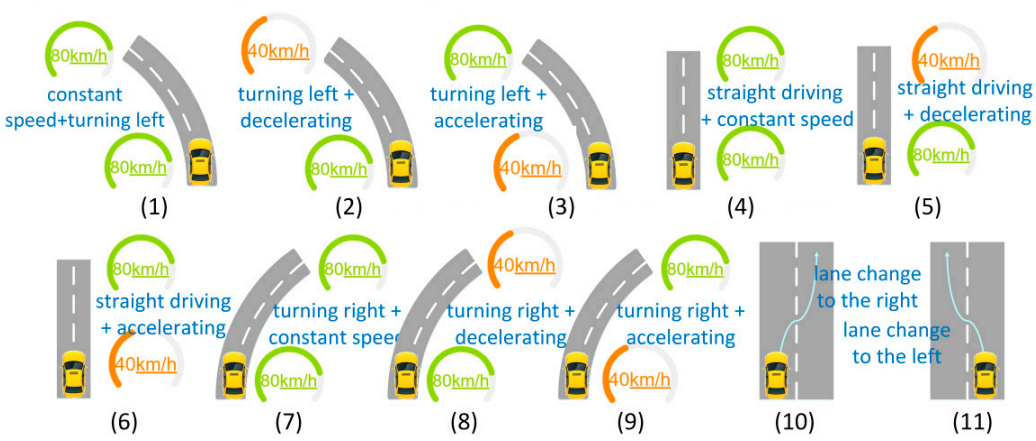


Figure 2. Eleven basic vehicle behaviors.

The typical micro-behavior data collected is shown in Figure 3. The accelerations and speed change over time while the vehicle runs. In Figure 3, the segment where acceleration only changes slightly may represent an L&C driving behavior (Segment 1), whereas the segment with violent acceleration change may mean that the vehicle is taking an accelerating behavior (Segment 2). The purpose of expressing vehicle behavior is to identify what behavior the vehicle is taking in a specific segment based on microscopic data. The expression of vehicle behavior consists of two steps: (1) automatic segmentation, i.e., extracting time series segments of basic vehicle behavior from the entire time series, and (2) behavior identification, i.e., identifying the extracted vehicle behavior time series segments.

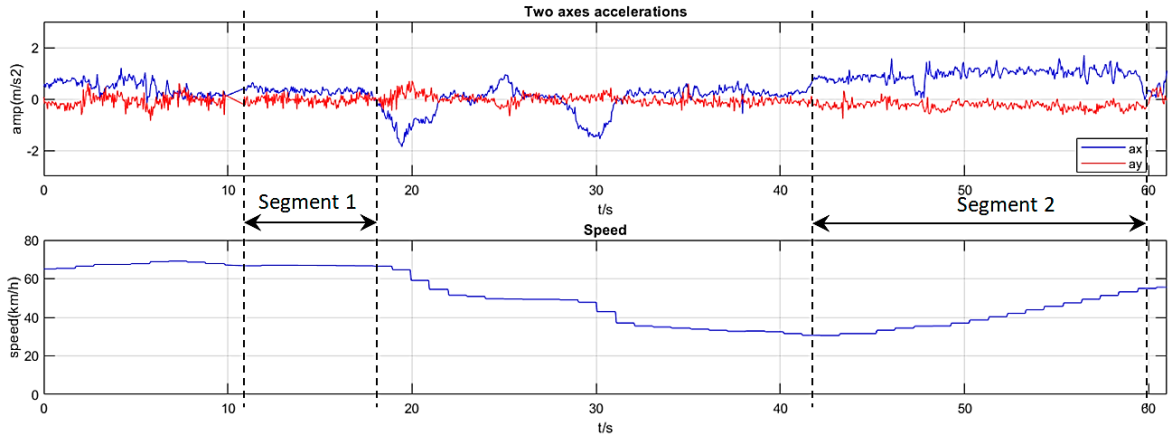


Figure 3. Typical micro−behavior data sample.

3.1.1. Automatic Segmentation

For vehicle behaviors, accelerating, decelerating, and turning have more significant data features than L&C. After these unique behavior segments are extracted, the rest are L&C vehicle behavior segments. Thus, the critical point of vehicle behavior time series segmentation is to extract the accelerating, decelerating, and turning segments. This paper defines these key segments as segments of interest (SOIs) for convenience. A short-time average energy (STAE) based one-parameter bi-threshold endpoint detection technology is used to carry out the automatic segmentation and extract the SOIs. Since this method was introduced in detail in [2], please refer to the paper for more details. A brief introduction to the main processes is presented as follows.

Let $y_i(n)$ be the time series segment of the ith frame obtained by framing the time series $x(n)$, then the STAE $E(i)$ of $y_i(n)$ can be calculated as Equation (1):

$$E(i) = \sum_{n=0}^{L-1} y_i^2(n) \,, \qquad 1 \le i \le f_n \tag{1}$$

where f_n is the total number of frames after the time series framing, and L is the frame length.

Taking the longitudinal acceleration ax as an example, as shown in Figure 4, Figure 4a shows the change of ax with time when a vehicle gets close to a work zone, and Figure 4b shows the corresponding change of the STAE of ax. As seen from Figure 4b, some sections fluctuate greatly, meaning that the vehicle takes some behaviors (such as deceleration) there. To extract the section with significant fluctuation, a higher threshold of T2 is set, then the sections, i.e., the ones between C and D, with acceleration larger than T2 are SOIs. A lower threshold, T1, is used to find the finer start and end points of this SOI. The segment between the green vertical solid line and the red vertical dashed line in Figure 4a can be extracted by the endpoint detection method, i.e., the one between B and E.

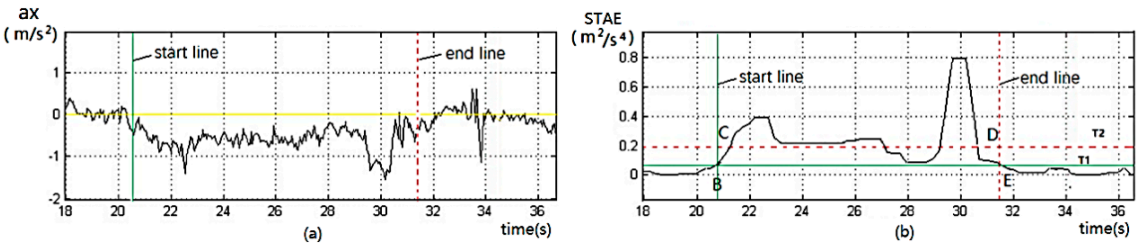


Figure 4. Demonstration of the STAE−based one−parameter−bi−threshold endpoint detection: (**a**) change of ax with time; (**b**) corresponding change of the STAE of ax with time.

The key to the endpoint detection is setting two thresholds, T1 and T2, i.e., the green horizontal solid line and the red horizontal dashed line in Figure 4b, respectively. An adaptive method is used in this research, i.e., taking values based on the behavior data characteristics of each vehicle itself. This research takes 40% and 60% of the maximum acceleration of the vehicle behavior data as the value of T1 and T2, respectively, which is the experience gained by several rounds of attempts. In fact, some heuristic algorithms can realize the automatic setting of threshold, but since this is not the focus of this research, it will not be discussed further. This method can shield the difference between vehicles and guarantee that SOIs be extracted in any condition.

Automatic segmentation is applied separately to the x-axis acceleration and y-axis acceleration time series. After the segmentation, two different sets of schemes will be generated, e.g., the green x-axis acceleration segmentation scheme and the red y-axis acceleration segmentation scheme, as shown in Figure 5. There are overlapping segments, and their unique segments correspond to different vehicle behavior of the actual driving process. For example, a segment with only a large x-axis acceleration may represent a linear accelerating behavior, a segment with only a large y-axis acceleration may represent a turning with constant speed behavior, and both may represent a decelerating turning. After SOIs are extracted using the automatic segmentation technique mentioned above, the remaining segments are L&C vehicle behavior.

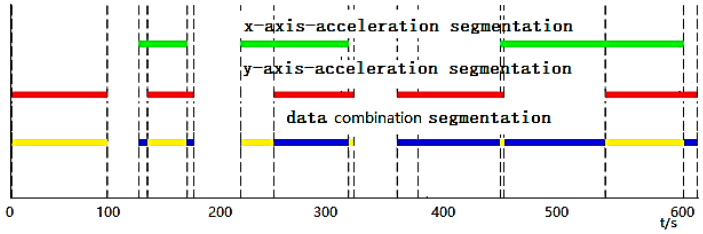


Figure 5. Data combination process.

It can be seen that through the automatic segmentation and data combination, the vehicle behavior time series can be divided into two categories: L&C and SOIs. The SOIs include 10 sub-categories (i.e., L&A, L&D, TL&A, TR&A, TL&C, TR&C, TL&D, TR&D, TL&CL, TR&CL) and need to be further divided by the vehicle behavior identification method.

3.1.2. Vehicle Behavior Identification

Identification belongs to the classic classification and clustering problem in machine learning. There is much existing research in this field, and many methods, including SVM and k-nearest neighbors (k-NN), have shown excellent performance [17,26,27]. The SVM-based vehicle behavior identification method is adopted in this research.

As a tool for solving classification, regression, and novelty detection problems, the SVM is already a proven method with good generality, robustness, high efficiency, simple calculation, and perfect theory. It has been widely involved in various research [32].

In brief, the theory of SVM is as follows [33]: assume that the input dataset is represented by N n-dimensional data points $\vec{x}_1, \vec{x}_2, ..., \vec{x}_N \in R^n$ and corresponding labels $y_1, y_2, ..., y_N \in \{-1, +1\}$. The main idea of SVM is to map each point $\vec{x}_i$ from the input space R^n to the feature space H by means of the mapping function $\phi(\vec{x}_i)$ and find a hyper-plane (Equation (2)) as the decision boundary so that the geometric margins between different categories are maximized or equivalently, the multiplicative inverse is minimized (Equation (3)).

$$\begin{gathered} \vec{w} \cdot \phi(\vec{x}) + b = 0 \\ subject\ to\ y_i(\vec{w} \cdot \phi(\vec{x}_i) + b) \geq 1, \quad \forall i \end{gathered} \tag{2}$$

where $\vec{w}$ is a vector perpendicular to the decision surface and b is a scalar (decision surface bias).

$$\begin{gathered} \min_{\lambda}(\tfrac{1}{2}\sum_{j,k=1}^{N} \lambda_j \lambda_k y_j y_k K(\vec{x}_j, \vec{x}_k) - \sum_{j=1}^{N} \lambda_i) \\ subject\ to \sum_{i=1}^{N} \lambda_i y_i = 0\ and\ 0 \leq \lambda_i \leq C\ \ \forall i \end{gathered} \tag{3}$$

where $\lambda = (\lambda_1, ..., \lambda_N)$ is the Lagrange multiplier, and C is a constant parameter that determines the trade-off between the maximum margin and minimum classification error. $K(.,.)$ is a kernel function.

Then SVM is able to classify any input $\vec{x}$ using the function of Equation (4).

$$f(\vec{x}) = sign(\vec{w} \cdot \phi(\vec{x}) + b) = sign(\sum_{j=1}^{N} \lambda_j y_j K(\vec{x}_j, x) + b) \tag{4}$$

In this research, the SVM is used to identify the SOIs extracted by the automatic segmentation technology as L&A, L&D, TL&A, TR&A, TL&C, TR&C, TL&D, TR&D, TL&CL, and TR&CL. The key to establishing a good SVM identification model lies in the training and testing data collection and feature selection. More details will be introduced in the Example part of this paper.

3.1.3. Evasive Behavior Judgment

Using automatic segmentation and vehicle behavior identification, the whole driving process of a vehicle can be decomposed into independent vehicle behavior segments,

some of which belong to normal vehicle behavior and some to evasive behavior. Those evasive behaviors are traffic conflict segments according to the definition of traffic conflict based on evasive behavior. This study uses a simple but effective threshold method to extract these evasive behaviors. As shown in Table 1, a previous study shows that when the longitudinal acceleration is larger than 3.92 m/s^2, or the longitudinal deceleration is smaller than -3.92 m/s^2, or the lateral acceleration is larger than 5.39 m/s^2, the behavior can be considered as evasive [34]. Therefore, judging each behavior segment one by one, if any acceleration value in the segment exceeds the threshold value in Table 1, the segment can be determined as an evasive behavior.

Table 1. Evasive behavior judgment based on acceleration (m/s^2).

Acceleration	Longitudinal Deceleration	Longitudinal Acceleration	Lateral Acceleration
Judgment	<−3.92	>3.92	>5.39

3.2. Proximity-Based Analysis

Proximity-defined-based TCT is classical, and the SSAM is the most influential analysis framework. Detailed information on the SSAM can be found in [9]. This study also uses the SSAM to detect two and multi-vehicle conflicts. Considering the completeness of the content of this paper, the SSAM method will be introduced as follows briefly.

The SSAM detects traffic conflicts by analyzing the trajectory (TRJ) output files of simulation software, such as Vissim, Aimsun, Paramics, and TEXAS. The workflow of the SSAM is shown in Figure 6 [9]. It should be noted that although the SSAM was initially proposed for simulation software, it can also be used for measured data in practice. By organizing the measured data according to the format of TRJ files, it can be input into the SSAM for analysis.

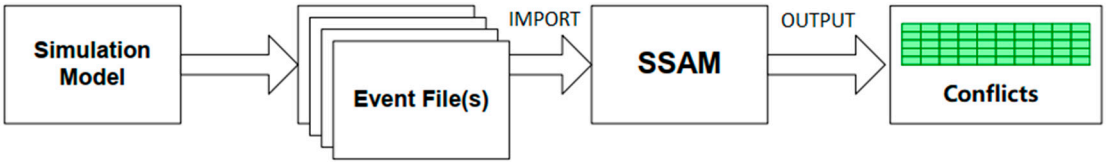


Figure 6. Workflow of SSAM.

The SSAM can output rich indicators for each traffic conflict, such as Time to Collision (TTC), Post-Encroachment Time (PET), Deceleration Rate (DR), Location of the Conflict Point (LCP), etc. The theory of the model and the calculation method for the key indicators are briefly explained by taking the cross conflict between the left-turning vehicle A and the straight-running vehicle B as an example, as shown in Figure 7. The analysis process includes the following three steps:

(1) The SSAM constructs a zone grid to cover the entire rectangular analysis area. Individual square zones cover 15.25 m by 15.25 m areas. The SSAM projects the trajectory (including vehicle speed, acceleration, and other information) output by the simulation software to the grid.

(2) Let (x_{Ai}, y_{Ai}) and (x_{Bi}, y_{Bi}), v_{Ai} and v_{Bi}, a_{Ai} and a_{Bi} be the position coordinates, speed, and acceleration of vehicles A and B at time step t_i (i = 1, 2, 3,...), respectively. Wherein t_1 is the time when vehicle A or vehicle B takes measures to avoid a crash. For vehicle A, according to the set of TTC threshold, calculate the distance that the vehicle does not take any measure and keeps the speed v_{A1} within the $TTC_{threshold}$ as $DIS_1 = v_{A1} \cdot TTC_{threshold}$. Since the time is very short, the actual distance traveled by the vehicle can be approximately expressed as $DIS_2 = \sqrt{(x_{A1} - x_{A2})^2 + (y_{A1} - y_{A2})^2}$. If $DIS_2 < DIS_1$, then let $DIS_1 = DIS_1 - DIS_2$, where $DIS_2 = \sqrt{(x_{A3} - x_{A2})^2 + (y_{A3} - y_{A2})^2}$.

Repeat this step until $DIS_2 > DIS_1$. As shown in Figure 7, it is assumed that the requirements are met in the S_3 segment. Use the same method to process the driving trajectory of vehicle B, assuming that the requirements are met in the Q_2 segment.

(3) Check whether an overlapping area exists between S_3 and Q_2. If not, the conflict will not be recorded. If there is an overlap, record the time t_A and t_B when vehicles A and B run to the conflict point, respectively; calculate the time t_{A1} and t_{B1} when vehicles A and B run to the conflict point with v_{A1} and v_{B1}, respectively; the TTC and PET can be calculated as TTC = min ($t_{A1} - t_1$, $t_{B1} - t_1$), PET = $|t_A - t_B|$.

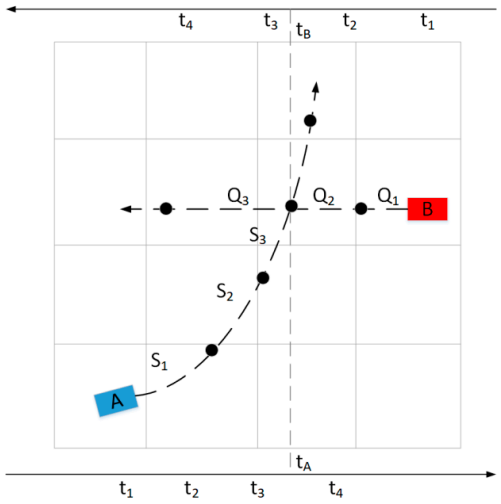


Figure 7. Demonstration of SSAM.

According to the angle θ between vehicles' driving directions when traffic conflict happens, the SSAM divides traffic conflicts into three types (as shown in Figure 8), i.e., rear-end conflict ($\theta < 30°$), lane change conflict ($30° \leq \theta \leq 85°$), and crossing conflict ($85° < \theta \leq 180°$).

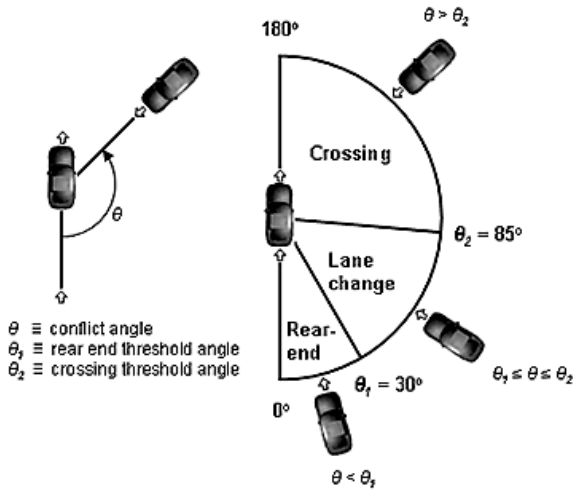


Figure 8. Demonstration of SSAM conflict types.

3.3. All Types of Conflict Analysis

Based on the vehicle micro-behavior data in the work zone, two sets of traffic conflict detection results can be obtained using the above two analysis methods. The results obtained by evasive behavior defined-based analysis include single-vehicle conflict, two and multi-vehicle conflict. In contrast, the examples obtained by proximity-defined-based analysis only include two and multi-vehicle conflicts. Therefore, for a conflict segment,

a straightforward way to identify its conflict type is to compare the two sets of detection results. If an evasive behavior segment is also in the detection result of the proximity-defined analysis, it can be judged as a two or multi-vehicle conflict. Otherwise, it is a single-vehicle conflict. In practice, this study matches the segments detected by the evasive behavior analysis method with the results detected by the proximity analysis method one by one. Many features can be used to match the two sets of results, including vehicle ID, time, and spatial location of conflict events. The flowchart of the matching process is shown in Figure 9. It is assumed that the data set of evasive behavior detection result is EvasiveDataSet, the data set of proximity detection result is PromixityDataSet, and the conflict type is conflictType.

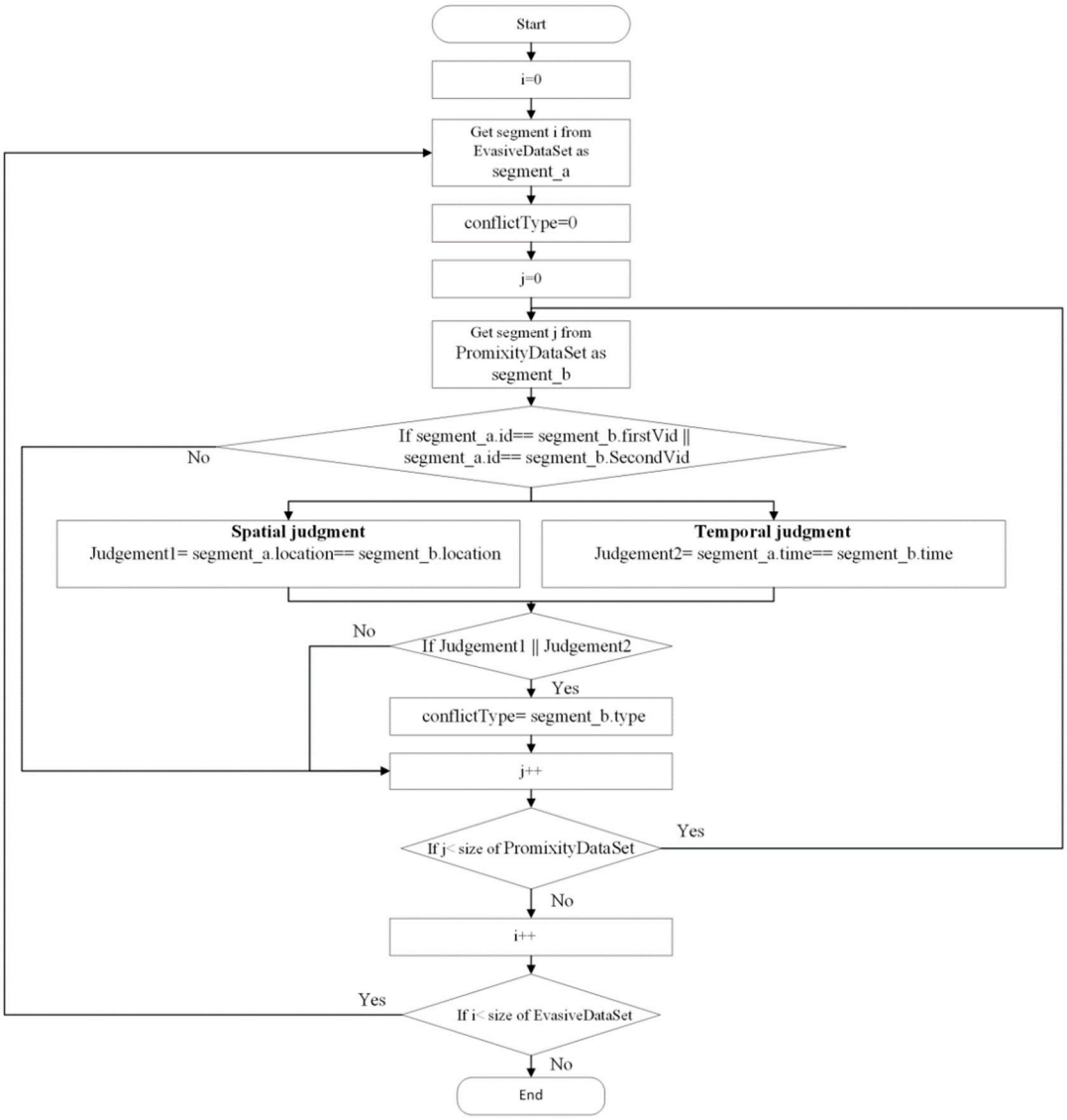


Figure 9. Flowchart of the matching process.

After the matching process, if the conflictType of a conflict segment is 0, it indicates that it is a single-vehicle conflict; otherwise, it is a two or multi-vehicle conflict, and its specific conflict type can be taken from the analysis results of the SSAM.

4. Example

In this section, a practical work zone is used as an example to demonstrate the implementation and effect of the method proposed in Section 3. The work zone is located on

the S20 expressway of Shanghai, as shown in Figure 10. The S20 is a two-way eight-lane expressway with a speed limit of 80 km/h. The maintenance task is to repair the pothole on the first and second lanes, and a traffic configuration of closing the first and second lanes and opening the third and fourth lanes is adopted. In this example, simulation is used to collect vehicle micro-behavior data. To restore the actual work zone scene as accurately as possible, the simulation model must be calibrated before the simulation data collection.

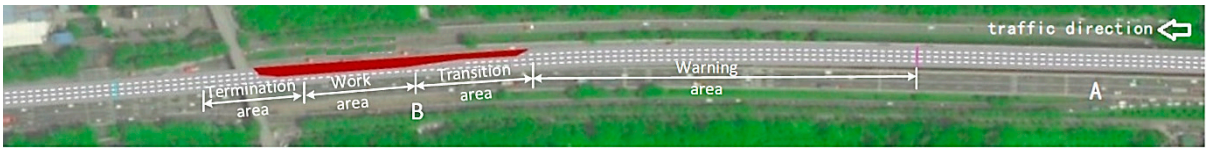


Figure 10. Spatial location and layout of the example work zone.

4.1. Data Acquisition

4.1.1. Model Calibration

Various parameters can be set in Vissim, and there is also a lot of research on parameter calibration. Usually, researchers choose to calibrate parameters such as standstill distance (CC0), gap time distribution (CC1), following distance oscillation (CC2), waiting time before diffusion, and minimum clearance [35]. After parameter adjustment, the actual traffic volume, speed, and speed distribution are compared with the simulated values to evaluate the effect of parameter adjustment. The parameters leading to the smallest error between the actual and simulated values are optimal parameters.

Data collection is carried out at positions A and B using advanced video detection devices to obtain the traffic volume, speed, and other data required for calibration. Position A is located 1 km upstream of the work zone, and the traffic flow is not affected by the work zone. Obtain the traffic volume and speed distribution at positions A and B by vehicle type. This study only distinguishes between small and large vehicles, in which small vehicles include cars, small and medium-sized buses, and small trucks, and large vehicles include large buses and large and medium-sized trucks. After continuously collecting the traffic flow data for 1 h, the speed distribution at positions A and B can be obtained, as shown in Tables 2 and 3. The traffic volume measured at position A is 3500 vehicles/hour, the proportion of large vehicles is 22%, and that of small vehicles is 78%. The average speed of the large vehicles at position B is 75.4 km/h, the average speed of the small vehicles is 76.4 km/h, and the average speed of all vehicles is 75.7 km/h.

Table 2. Speed distribution of small and large vehicles at position A.

Control Point (km/h)	35	45	55	65	75	80	85	90	95	100	105	110
Cumulative proportion of small vehicles	0	0.01	0.03	0.04	0.20	0.54	0.76	0.81	0.85	0.91	0.96	1
Cumulative proportion of large vehicles	0	0	0	0	0	0.05	0.43	0.8	0.88	0.95	0.98	1

Table 3. Speed distribution of small and large vehicles at position B.

Control Point (km/h)	35	45	55	65	75	80	85	90	95	100	105	110
Cumulative proportion of small vehicles	0	0.01	0.09	0.28	0.65	0.75	0.86	0.92	0.97	0.99	1	1
Cumulative proportion of large vehicles	0	0.02	0.07	0.30	0.63	0.74	0.84	0.89	0.93	0.95	0.98	1

Establish the simulation model in Vissim. Reconstruct the layout of the road and maintenance work zone according to the actual data. Set the input traffic volume as 3500 vehicles/h, with 22% for large vehicles and 78% for small vehicles. Set the expected speed distribution of large and small vehicles as the vehicle speed distributions at location A.

Taking the five parameters, i.e., CC0, CC1, CC2, waiting time before diffusion, and minimum clearance as factors, each factor considers four levels, and an L16(45) orthogonal experiment is designed. Change the driving behavior parameters according to the values in the orthogonal experiment and conduct 16 simulations. Each simulation measures the speed distribution and the average speeds of small, large, and all vehicles at location B for comparison with the collected data. Finally, it is found that when CC0 is taken as 1.5, CC1 as 0.7, CC2 as 4, the waiting time before diffusion as 80, and the minimum clearance as 0.5, the error between the simulation data and the actual data is the smallest. ANOVA also shows no significant difference between the simulation and actual data ($p > 0.05$); thus, the calibration met the requirements.

4.1.2. Data Acquisition

Vissim can output detailed behavior data with the finest sampling frequency up to 20 Hz. However, the disadvantage is that it can only obtain the acceleration in the driving direction, i.e., the acceleration in the x direction, and is incapable of obtaining the acceleration in the lateral y direction. Therefore, a program is developed to solve the acceleration in two directions according to the vehicle's position. The basic principle is illustrated below.

Take (x, y) as the coordinate of the vehicle at time t, then the radius of curvature ρ of the trajectory at time t is:

$$\rho = \frac{(x'^2 + y'^2)^{\frac{3}{2}}}{x''y' - x'y''} \tag{5}$$

The speed at time t:

$$v = \sqrt{x'^2 + y'^2} \tag{6}$$

The longitudinal acceleration ax:

$$ax = \dot{v} = \frac{x'x'' + y'y''}{\sqrt{x'^2 + y'^2}} \tag{7}$$

The lateral acceleration ay:

$$ay = \frac{v^2}{\rho} = \frac{x''y' - x'y''}{\sqrt{x'^2 + y'^2}} \tag{8}$$

4.2. Evasive Behavior-Based Analysis

By implementing the above vehicle micro-behavior data acquisition algorithm and vehicle behavior automatic segmentation algorithm on the Matlab platform, the data output from Vissim can be divided into independent basic vehicle behavior segments. Additionally, the behavior types of these segments can be identified with the help of the vehicle behavior identification model. This part will focus on establishing a vehicle behavior identification model based on the SVM.

4.2.1. SVM-Based Vehicle Behavior Identification Model Establishment

(1) Data acquisition

The establishment of the SVM identification model requires training data and testing data. In the simulation environment, data acquisition is relatively easy. A large amount of data can be obtained by changing the simulation seed and running it many times. It is worth noting that in the simulation process, the vehicle ID should be presented through the setting of visual parameters, and the simulation process should be recorded to facilitate the annotation of vehicle behavior types in the later steps. Different vehicle behavior segments can be extracted through the automatic segmentation of vehicle behavior. These segments contain vehicle ID, running time, vehicle location, and other information. The actual

vehicle behavior types corresponding to these segments can be determined by reviewing the videos recorded during the simulation process. A total of 328 valid segments were obtained, including 46 L&C, 36 L&A, 20 L&D, 62 TR&C, 38 TR&A, 14 TR&D, 47 TL&C, 36 TL&A, 11 TL&D, 9 TL&CL, and 9 TR&CL.

(2) Features

Data from 11 types of vehicle behaviors were collected through the training data acquisition process. Based on these data and many practical verifications, the following features are selected: ① the slope of the fitted line of the speed curve; ② the average value of ax; ③ the average value of the accelerations in the y direction that are greater than or equal to 0; ④ the average value of the accelerations in the y direction that are less than or equal to 0; ⑤ the slope of the fitted line of the ay curve; ⑥ the absolute value of the ratio of the sum of all non-negative accelerations in the y direction to the sum of all non-positive accelerations; and ⑦ the absolute value of the ratio of the sum of all non-positive accelerations in the y direction to the sum of all non-negative accelerations.

(3) Training and verification

Many off-the-shelf SVM toolkits are available, and the LibSVM package is one of the most swell known packages [36]. The LibSVM package provides a number of kernel functions, including the linear function, polynomial function, radial basis function (RBF), and sigmoid kernel function. The RBF is used in this paper after trials, with two parameters, i.e., the penalty parameter C and the kernel coefficient γ, to be tuned. In this paper, the cross-validation and grid search techniques are used to obtain the optimal values of the parameters. The data analysis process in this paper was operated on Matlab. For a detailed algorithm, please refer to [36].

The 328 groups of data are divided into a training set and a test set in a ratio of 3:1. Using the normalized function mapminmax of Matlab, the training data set was normalized to the [0, 1] interval. Using the cross-validation and grid search methods, it is found that when C = 1, γ = 4, the best accuracy can be achieved at 90.1%, thus, verifying that the SVM model works well in behavior identification.

4.2.2. Distribution of Evasive Behavior

Apply the above-trained identification model to all vehicle behavior segments to recognize them as one of 11 basic behavior types. Then, iterate each vehicle behavior segment and judge whether the lateral or longitudinal acceleration exceeds the threshold in Table 1. If so, the behavior can be considered evasive; otherwise, it can be regarded as normal.

In this example, the complete micro-behavior data of 546 vehicles are collected, and is divided into 1913 behavior segments, including 313 L&Cs (16%), 267 TL&Cs (14%), 266 TR&As (14%), 240 L&As (13%), 194 TR&Cs (10%), 172 TL&As (9%), 149 L&Ds (8%), 121 TL&Ds (6%), 65 TR&Ds (4%), 64 TR&CLs (3%), and 62 TL&CLs (3%).

A total of 32 evasive behaviors were detected, including seven TR&Ds (22%), two TL&Ds (6%), and 23 L&Ds (72%). Figure 11 shows the thermal diagram of these evasive behaviors, which can intuitively display their spatial distribution within the work zone. It can be seen that these evasive behaviors are mainly distributed in the warning area and upstream transition area of the work zone.

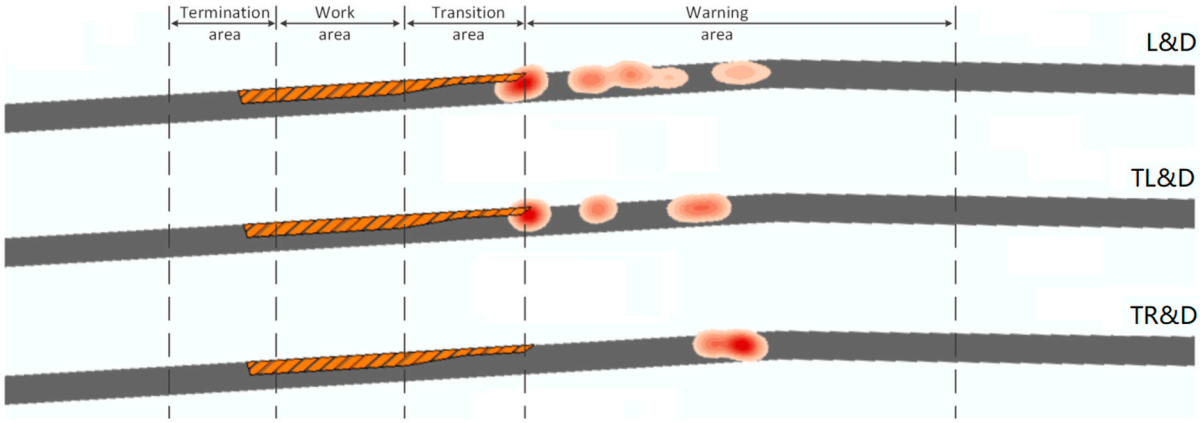


Figure 11. Spatial distribution of evasive behavior.

4.3. SSAM Analysis

Inputting the TRJ file from Vissim into the SSAM, 26 traffic conflicts can be obtained, including 18 rear-end conflicts and eight lane-changing conflicts. Figure 12 shows the thermal diagram of these conflicts. It can be seen that these traffic conflicts are mainly distributed in the warning area and upstream transition area of the work zone. Taking the threshold in Table 1 as the judgment and the DR of the SSAM as the factor, it is found that only three show evasive behavior, which shows that not all two and multi-vehicle conflict processes show evasive behavior.

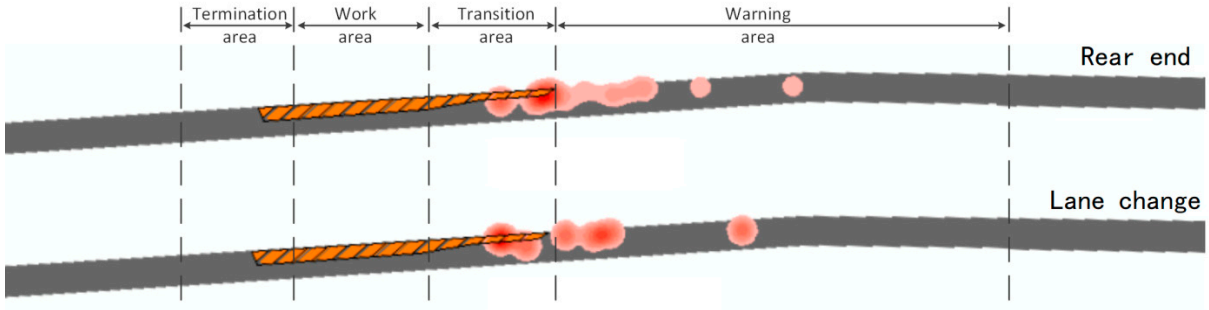


Figure 12. Distribution of SSAM traffic conflicts.

4.4. All Types of Conflict Analysis

Implement the code in Section 3.3 on the Matlab platform, and the following results can be obtained. Of the 32 evasive behaviors, 11 are also included in the results of the SSAM analysis, of which six are rear-end conflicts, and five are lane change conflicts. These behavior segments can be determined as two or multi-vehicle conflicts, and the remaining 21 can be determined as single-vehicle conflicts. Therefore, the all-types of conflict analysis result contains 21 single-vehicle conflicts (45%) and 26 two or multi-vehicle conflicts (55%). Among the 21 single-vehicle conflicts, 15 are L&Ds (71%), five are TL&Ds (24%), and one is TR&D (5%). Among the 26 two and multi-vehicle conflicts, 18 are rear-end conflicts (69%), and eight are lane-changing conflicts (31%).

Many studies have verified the effectiveness of using the SSAM to detect two-vehicle and multi-vehicle conflicts [9]. Therefore, to verify the effectiveness of this method in all types of conflict detection, we only need to verify the accuracy of single-vehicle conflict detection. The following method is adopted: compare the number of single-vehicle conflicts detected automatically with the number of single-vehicle conflicts obtained from manual analysis of simulation video data. The results show that 19 of the 21 single-vehicle conflicts are truly single-vehicle conflicts through manual judgment; the accuracy of the automatic single-vehicle conflict detection algorithm is as high as 90%. It is worth noting that two

two-vehicle conflicts are detected as single-vehicle conflicts, which may be caused by the failure of automatic segmentation to extract complete fragments of vehicle conflicts. Therefore, a more comprehensive automatic segmentation method should be studied in further research.

It can be seen that the method proposed in this paper can detect all types of traffic conflicts, which makes up for the limitation that traditional TCT can only detect the conflict between two or more vehicles. Given a behavior segment, it can be matched as single vehicle conflict, two or multi-vehicle conflict. Single-vehicle conflict can be further divided into 10 types, such as L&A, L&D, and TL&D. In contrast, two and multi-vehicle conflicts can be further divided into rear-end conflict, lane-change conflict, and crossing conflict.

4.5. Applicability Analysis

Next, this study will further verify the applicability of this method in different scenarios with the help of simulation. For length reasons, this paper only studies scenarios under different traffic volumes. As shown in Table 4, Scenario 4 is the basic scenario (same as the above example), and only traffic volume differs from the basic scenario for each of the other scenarios. For each scenario, the experiment is conducted three times.

Table 4. Traffic volume configuration.

Scenario	1	2	3	4	5
Traffic volume	2000	2500	3000	3500	4000

After the experiments, the data is analyzed, and the results shown in Table 5 are obtained. Taking the second experiment (i.e., Experiment 8) with a traffic volume of 3000 vehicles/h as an example, the SSAM analysis detected eight traffic conflicts, including six rear-end conflicts and two lane-change conflicts, of which two showed evasive behavior. The analysis of evasive behavior detected 24 evasive behaviors, including seven TR&D, three TL&D, and 14 L&D. The all-types of conflict analysis found that four evasive behaviors appeared in the results of the SSAM analysis, of which three were rear-end conflict and one was lane change conflict. Therefore, 20 single-vehicle conflicts were finally detected.

The classical Poisson regression model [37] is carried out with the traffic volume as the independent variable, the number of traffic conflicts detected by the SSAM, and the number of single-vehicle conflicts as dependent variables, respectively. The regression result for the SSAM-traffic volume is shown in Table 6. It can be seen that at the significance level of 0.05, the likelihood ratio test passes, and the model is valid. The intercept and the coefficient of traffic volume have statistical significance when the significance level is 0.01. The coefficient of traffic volume is larger than 0, which indicates that with the increase in traffic volume, the number of traffic conflicts detected by the SSAM will also increase. MacFadden R^2 is 0.893, which means that the traffic volume can explain 89.3% of the change of the dependent variable. The final regression equation can be written as $Ln\ SSAM = 0.003 \times Traffic\ volume - 6.316$. The regression result for single vehicle conflict-traffic volume is shown in Table 7. It can be seen that at the significance level of 0.05, the likelihood ratio test passes, and the model is valid. The coefficient of traffic volume has statistical significance when the significance level is 0.01, and the intercept has statistical significance when the significance level is 0.05. The coefficient of traffic volume is larger than 0, which indicates that with the increase in traffic volume, the number of single-vehicle conflicts will also increase. MacFadden R^2 is 0. 687, which means that the traffic volume can explain 68.7% of the change of the dependent variable. The final regression equation can be written as $Ln\ \ Singlevehicleconflict = 0.001 \times Traffic\ \ volume - 0.677$.

Table 5. Results of the experiments.

Scenario, Traffic Volume (Vehicles/h)		Scenario 1, 2000			Scenario 2, 2500			Scenario 3, 3000			Scenario 4, 3500			Scenario 5, 4000		
Experiment		**1**	**2**	**3**	**4**	**5**	**6**	**7**	**8**	**9**	**10**	**11**	**12**	**13**	**14**	**15**
SSAM	rear end	0	0	1	0	2	2	1	6	6	18	13	13	65	75	103
	lane change	0	0	0	3	3	0	1	2	2	8	5	5	17	25	20
	total	0	0	1	3	3	2	2	8	8	26	18	18	82	100	123
	evasive DR	0	0	0	2	1	0	1	2	2	3	6	8	14	22	25
Evasive behavior	total	9	11	5	12	15	7	13	24	10	32	36	36	76	90	106
	TR&D	1	2	1	3	4	3	3	7	3	7	6	9	15	21	17
	TL&D	0	3	0	1	2	1	1	3	1	2	4	8	8	11	16
	L&D	6	2	3	5	7	3	7	14	6	23	21	19	52	58	73
	TR&A	0	0	0	1	1	0	2	0	0	0	3	0	1	0	0
	TR&C	2	3	1	2	0	0	0	0	0	0	2	0	0	0	0
	TL&CL	0	1	0	0	1	0	0	0	0	0	0	0	0	0	0
All type conflicts	total	9	11	5	12	15	7	13	24	10	32	36	36	76	90	106
	Rear end (R)	0	0	0		1	0	0	3	3	6	3	6	11	22	27
	Lane change (L)	0	0	0	1	1	0	0	1	0	5	2	0	2	8	6
	R + L	0	0	0	1	2	0	0	4	3	11	5	6	13	30	33
	single	9	11	5	11	13	7	13	20	7	21	31	30	63	60	73

Table 6. Poisson regression result for SSAM-traffic volume.

	Coefficients
Traffic volume	0.003 ** (17.882)
Intercept	−6.316 ** (−10.775)
Sample size	15
Likelihood ratio test	χ^2 (1) = 676.170, p = 0.000
McFadden R^2	0.893

Dependent variable: number of traffic conflicts detected by SSAM; ** $p < 0.01$; z statistics in parentheses.

Table 7. Poisson regression result for single vehicle conflict -traffic volume.

	Coefficients
Traffic volume	0.001 ** (13.326)
Intercept	−0.677 * (−2.124)
Sample size	15
Likelihood ratio test	χ^2 (1) = 218.075, p = 0.000
McFadden R^2	0.687

Dependent variable: number of single-vehicle conflicts; * $p < 0.05$; ** $p < 0.01$; z statistics in parentheses.

Linear regression is used to show the relationship between the number of evasive behaviors and the number of traffic conflicts detected by the SSAM, as shown in Table 8. The R^2 reaches 0.972, which means that the number of evasive behaviors can explain 97.2%

of the change of the dependent variable; at the significance level of 0.05, the F test passes, and the model is valid; the intercept and independent variable coefficient are statistically significant at the significance level of 0.01. The independent variable coefficient >0 indicates that with the increase of the number of evasive behaviors, the number of traffic conflicts detected by the SSAM will also increase; the final regression equation can be written as $SSAM = 1.231 \times Number\ of\ evasive7\ behaviour - 13.296$.

Table 8. Linear regression result for SSAM -evasive behavior.

	Coefficients
Constant	−13.296 ** (−5.068)
Evasive behavior	1.231 ** (21.063)
n	15
R^2	0.972
Adj. R^2	0.969
F Value	F (1,13) = 443.654, p = 0.000

Dependent variable: number of traffic conflicts detected by SSAM; D-W: 1.680; ** $p < 0.01$; t statistics in parentheses.

It can be seen that:

(1) With the increase of traffic volume, the number of single-vehicle conflicts, two and multi-vehicle conflicts will increase. This is in line with previous research results [38] and verifies this method's applicability in different traffic scenarios.

(2) Regression analysis shows a significant correlation between the total number of SSAM traffic conflicts and the number of evasive behaviors. The analysis method based on evasive behavior does have the connotation of single-vehicle, two, and multi-vehicle conflict; thus, the number of evasive behaviors can be used to predict the number of traffic conflicts.

(3) When the traffic volume is low, the SSAM method cannot detect any traffic conflict, but the evasive behavior analysis can detect the single vehicle conflict. Therefore, there is a deficiency in only using the SSAM method in the safety assessment for work zones. Additionally, it is not enough to only analyze evasive behavior, for although the evasive behavior includes some two and multi-vehicle conflicts, it only consists of the traffic conflicts showing evasive behavior.

In addition, two interesting aspects can be further discussed:

(1) In Table 5, R + L is the number of evasive behaviors which also exist in the SSAM analysis results, that is, the number of two and multi-vehicle conflicts showing evasive behavior. Theoretically, this value should be greater than or equal to the value of evasive DR. Each conflict in the SSAM detection results includes two or multiple vehicles. When the DR of the conflict exceeds the threshold, it indicates that at least one vehicle shows evasive behavior. Evasive behavior is analyzed for each vehicle, so the results should include the evasive behaviors of all vehicles. However, the above results are not completely consistent, mainly because there may be errors in automatic segmentation and behavior identification, which can be improved by improving the segmentation method and identification rate in further research.

(2) The total number of traffic conflicts detected by the SSAM should be greater than or equal to R + L because two and multi-vehicle conflicts also include those that do not show evasive behavior. This can be seen from the fact that the number of evasive DR is not equal to the total number of conflicts detected by the SSAM. This conclusion can also be verified by the theory of the SSAM. When detecting traffic conflict, the SSAM takes TTC and PET as the judgment. When either is less than a certain threshold, the situation can be regarded as a traffic conflict, which is not directly related to DR.

Therefore, the detection results include vehicles with evasive behavior and vehicles with normal behavior.

5. Summary and Outlook

Serious safety problems exist in work zones. Current conflict detection methods only focus on two and multi-vehicle conflicts and cannot detect single-vehicle conflicts, but single-vehicle conflicts often occur in work zones. This study integrates the definitions of traffic conflict based on evasive behavior and based on proximity and puts forward an all-type of traffic conflict detection method. The two and multi-vehicle conflict is analyzed by the classic SSAM method, and single-vehicle conflict is detected mainly by the vehicle behavior analysis method. Through automatic segmentation, the SVM-based vehicle behavior identification, and threshold judgment methods, 10 types of evasive behavior can be detected. After removing the segments contained in the SSAM analysis results, they are all single vehicle conflicts. Then, taking an actual work zone as an example, the implementation and effect of this method are demonstrated, and its feasibility in all types of traffic conflict detection is verified. Finally, taking the traffic volume as the factor, the applicability of this method in multiple scenarios is studied.

The method proposed in this study can identify single vehicle conflicts, but it only focuses on the number of conflicts, and the severity of conflicts is not considered. For example, for two evasive L&Ds, this study does not consider their relative seriousness. Further analysis can consider indexes such as jerk as the severity judgment. This paper only discusses the applicability of the method under different traffic volumes. Later study can further explore the applicability under the action of more factors, such as the proportion of large vehicles, and the layout of the work zone, etc. The vehicle behavior data in the example is collected by simulation. Further studies can obtain data from other technologies to verify the simulation results. Finally, the number of single vehicle conflicts detected by the method proposed in this paper is closely related to the threshold selection. Considering that this paper mainly focuses on conflict detection and the evaluation criterion is beyond the scope of this study; the threshold set in this paper only refers to the existing research. Further study should determine a more realistic threshold in combination with the evaluation criterion.

Author Contributions: Conceptualization, Z.X. and D.C.; methodology, Z.X.; software, Z.X.; validation, Z.X. and D.C.; formal analysis, Z.X.; investigation, Z.X.; resources, Z.X.; data curation, Z.X.; writing—original draft preparation, Z.X.; writing—review and editing, D.C.; visualization, D.C.; supervision, D.C.; project administration, D.C.; funding acquisition, D.C. All authors have read and agreed to the published version of the manuscript.

Funding: This research was funded by the Science and Technology Commission of Shanghai Municipality under Grant No. 20090503100.

Data Availability Statement: The data used to support the findings of this study are included within the article.

Conflicts of Interest: The authors declare no conflict of interest.

References

1. Laureshyn, A.; Várhelyi, A. *The Swedish Traffic Conflict Technique: Observer's Manual*; Lund University: Lund, Sweden, 2018.
2. Xu, Z.; Yang, Q. Novel fast safety assessment method for the buffer section of maintenance work zone. *IET Intell. Transp. Syst.* **2019**, *13*, 773–779. [CrossRef]
3. Zheng, L.; Ismail, K.; Meng, X. Traffic conflict techniques for road safety analysis: Open questions and some insights. *Can. J. Civ. Eng.* **2014**, *41*, 633–641. [CrossRef]
4. Mahmud, S.S.; Ferreira, L.; Hoque, S.; Tavassoli, A. Micro-simulation modelling for traffic safety: A review and potential application to heterogeneous traffic environment. *IATSS Res.* **2019**, *43*, 27–36. [CrossRef]
5. Meng, Q.; Weng, J. Evaluation of rear-end crash risk at work zone using work zone traffic data. *Accid. Anal. Prev.* **2011**, *43*, 1291–1300. [CrossRef]
6. Park, H.; Oh, C.; Moon, J.; Kim, S. Development of a lane change risk index using vehicle trajectory data. *Accid. Anal. Prev.* **2018**, *110*, 1–8. [CrossRef]

7. Meng, X.; Zheng, L.; Bi, H.; Guan, Z.; Xu, H. Research on Traffic Characteristics and Traffic Conflicts of One-way Closed Work Zone on Expressway. *China J. Highw. Transp.* **2013**, *26*, 140.
8. Mahmud, S.; Ferreira, L.; Hoque, M.; Tavassoli, A. Reviewing traffic conflict techniques for potential application to developing countries. *J. Eng. Sci. Technol.* **2018**, *13*, 1869–1890.
9. Gettman, D.; Head, L. Surrogate safety measures from traffic simulation models. *Transp. Res. Record* **2003**, *1840*, 104–115. [CrossRef]
10. Tang, C.; Zhang, T.; He, Y. *Road Safety Assessment*; China Communication Press Co., Ltd.: Beijing, China, 2008; Available online: http://product.dangdang.com/11037415383.html (accessed on 29 October 2022).
11. Allen, B.L.; Shin, B.T.; Cooper, P.J. *Analysis of Traffic Conflicts and Collisions*; Transportation Research Board: Washington, DC, USA, 1978.
12. Ishak, S.; Qi, Y.; Rayaprolu, P. Safety Evaluation of Joint and Conventional Lane Merge Configurations for Freeway Work Zones. *Traffic Inj. Prev.* **2012**, *13*, 199–208. [CrossRef]
13. Zaki, M.H.; Sayed, T.; Shaaban, K. Use of drivers' jerk profiles in computer vision–based traffic safety evaluations. *Transp. Res. Record* **2014**, *2434*, 103–112. [CrossRef]
14. Bagdadi, O.; Várhelyi, A. Development of a method for detecting jerks in safety critical events. *Accid. Anal. Prev.* **2013**, *50*, 83–91. [CrossRef] [PubMed]
15. Xu, Z.; Yang, Q. Fast Safety Assessment and Correction Framework for Maintenance Work Zones. *arXiv* **2019**, arXiv:1911.01179.
16. Hu, X. A video-based Technology to Identify and Determine the Traffic Conflict at the Intersection. Master's Thesis, North China University of Technology, Beijing, China, 2013.
17. Zhang, F. Study on a Computer Vision System for Detecting Traffic Conflict between Vehicles at Intersections. Master's Thesis, Tongji University, Shanghai, China, 2008.
18. Guo, Y.; Sayed, T.; Zaki, M.H.; Liu, P. Safety evaluation of unconventional outside left-turn lane using automated traffic conflict techniques. *Can. J. Civ. Eng.* **2016**, *43*, 631–642. [CrossRef]
19. Chen, A.Y.; Chiu, Y.-L.; Hsieh, M.-H.; Lin, P.-W.; Angah, O. Conflict analytics through the vehicle safety space in mixed traffic flows using UAV image sequences. *Transp. Res. Part C: Emerg. Technol.* **2020**, *119*, 102744. [CrossRef]
20. Raju, N.; Arkatkar, S.; Joshi, G. Effect of Construction Work Zone on Traffic Stream Parameters Using Vehicular Trajectory Data under Mixed Traffic Conditions. *J. Transp. Eng. Part A Syst.* **2020**, *146*, 05020002. [CrossRef]
21. Iguernaissi, R.; Merad, D.; Aziz, K.; Drap, P. People tracking in multi-camera systems: A review. *Multimedia Tools Appl.* **2019**, *78*, 10773–10793. [CrossRef]
22. Fitch, G.M.; Hanowski, R.J. Using Naturalistic Driving Research to Design, Test and Evaluate Driver Assistance Systems. In *Handbook of Intelligent Vehicles*; Springer: London, UK, 2012; pp. 559–580.
23. Dingus, T.A.; Klauer, S.G.; Neale, V.L.; Petersen, A.; Lee, S.E.; Sudweeks, J.; Perez, M.A.; Hankey, J.; Ramsey, D.; Gupta, S. *The 100-Car Naturalistic Driving Study, Phase II-Results of the 100-Car Field Experiment*; Department of Transportation, National Highway Traffic Safety: Washington, DC, USA, 2006.
24. Eenink, R.; Barnard, Y.; Baumann, M.; Augros, X.; Utesch, F. UDRIVE: The European Naturalistic Driving Study. In Proceedings of the Transport Research Arena, IFSTTAR, TRA 2014, Paris, France, 14–17 April 2014.
25. Regan, M.A.; Williamson, A.; Grzebieta, R.; Charlton, J.; Lenne, M.; Watson, B.; Haworth, N.; Rakotonirainy, A.; Woolley, J.; Anderson, R. The Australian 400-car naturalistic driving study: Innovation in road safety research and policy. In Proceedings of the 2013 Australasian Road Safety Research, Policing & Education Conference, Brisbane, QLD, Australia, 28–30 August 2013; pp. 1–13.
26. Van Ly, M.; Martin, S.; Trivedi, M.M. Driver classification and driving style recognition using inertial sensors. In Proceedings of the 2013 IEEE Intelligent Vehicles Symposium (IV), Gold Coast, QLD, Australia, 23–26 June 2013; pp. 1040–1045.
27. Johnson, D.A.; Trivedi, M.M. Driving style recognition using a smartphone as a sensor platform. In Proceedings of the 2011 14th International IEEE Conference on Intelligent Transportation Systems (ITSC), IEEE, Washington, DC, USA, 5–7 October 2011; pp. 1609–1615.
28. Zheng, Y.; Hansen, J.H. Unsupervised driving performance assessment using free-positioned smartphones in vehicles. In *Proceedings of the 2016 IEEE 19th International Conference on Intelligent Transportation Systems (ITSC), Rio de Janeiro, Brazil, 1–4 November 2016*; Institute of Electrical and Electronics Engineers (IEEE): New York, NY, USA, 2016; pp. 1598–1603.
29. Abdulsattar, H.; Mostafizi, A.; Wang, H. Surrogate Safety Assessment of Work Zone Rear-End Collisions in a Connected Vehicle Environment: Agent-Based Modeling Framework. *J. Transp. Eng. Part A Syst.* **2018**, *144*, 04018038. [CrossRef]
30. Sankaran, B.; France-Mensah, J.; O'Brien, W.J. Integrating Activities Risk and Traffic Microsimulation Data for Temporal Risk Assessment in Construction Work Zones: A Proof of Concept. In Proceedings of the ASCE International Workshop on Computing in Civil Engineering 2017, Seattle, WA, USA, 25–27 June 2017; pp. 254–261.
31. So, J.J.; Dedes, G.; Park, B.B.; HosseinyAlamdary, S.; Grejner-Brzezinsk, D. Development and evaluation of an enhanced surrogate safety assessment framework. *Transp. Res. Part C Emerg. Technol.* **2015**, *50*, 51–67. [CrossRef]
32. Harrington, P. *Machine Learning in Action*; Simon and Schuster: New York, NY, USA, 2012.
33. Li, G.; Chung, W.-Y. Detection of driver drowsiness using wavelet analysis of heart rate variability and a support vector machine classifier. *Sensors* **2013**, *13*, 16494–16511. [CrossRef]

34. Wang, X.; Xing, Y.; Luo, L.; Yu, R. Evaluating the effectiveness of Behavior-Based Safety education methods for commercial vehicle drivers. *Accid. Anal. Prev.* **2018**, *117*, 114–120. [CrossRef]
35. Rrecaj, A.A.; Bombol, K.M. Calibration and Validation of the VISSIM Parameters-State of the Art. *TEM J.* **2015**, *4*, 255.
36. Chang, C.-C.; Lin, C.-J. LIBSVM: A library for support vector machines. *ACM Trans. Intell. Syst. Technol.* **2011**, *2*, 1–27. [CrossRef]
37. Lord, D.; Mannering, F. The statistical analysis of crash-frequency data: A review and assessment of methodological alternatives. *Transp. Res. Part A Policy Pract.* **2010**, *44*, 291–305. [CrossRef]
38. Gettman, D.; Pu, L.; Sayed, T.; Shelby, S.G.; Energy, S. *Surrogate Safety Assessment Model and Validation*; Turner-Fairbank Highway Research Center: McLean, VA, USA, 2008.